International Journal of Steel Structures (2019) 19(3):932–951
https://doi.org/10.1007/s13296-018-0176-x

Online ISSN 2093-6311
Print ISSN 1598-2351

Ultimate Behavior of Steel Cable-Stayed Bridges During Construction

Seungjun Kim[1] · Deokhee Won[2] · Young-Jong Kang[3]

Received: 9 April 2018 / Accepted: 15 October 2018 / Published online: 2 November 2018

Abstract
This paper presents an investigation of the ultimate behavior of steel cable-stayed bridges under construction. In general, cable-stayed bridges are subjected to quite large compressive forces induced by stayed cables, and may become unstable due to these excessive compressive forces, especially while under construction because of the characteristics of the general construction method. To investigate the ultimate behavior of steel cable-stayed bridges under construction, a three-step analysis, consisting of initial shape analysis, construction stage analysis and external load analysis, is proposed and used with considering various geometric and material nonlinearities of the structure, such as the cable-sag effect, beam-column effect of the girder and mast, large displacement effect and gradual yield effect. By performing extensive analytical study, the general ultimate behavior and mode are found and described in detail. Also, the effects of various geometric parameters on the ultimate behavior and load carrying capacity are studied, such as the cable-arrangement types, girder-mast flexural stiffness ratio and sectional area of stay cables.

Keywords Cable-stayed bridges · Nonlinear analysis · Initial shape analysis · Construction stage analysis · Ultimate analysis

1 Introduction

The cable-stayed bridge, a very popular bridge system for long-span bridges, consists of girder, mast and cables. The bridges are supported by the flexural strength and stiffness of the girder, compressive strength and stiffness of the mast, and tensile strength and stiffness of the stay cables. Because of their consistent combination, cable-stayed bridges show excellent structural efficiency while offering pleasing aesthetics.

While cable-stayed bridges show excellent structural efficiency, they do exhibit complex nonlinear characteristics (Adeli and Zhang 1995; Xi and Kuang 1999; Ren 1999; Freire et al. 2006). The first nonlinear factor is the cable-sag effect initiated by its own weight. The second factor is the beam-column effect of the girder and mast. The girder and mast of cable-stayed bridges are subjected to large compressive forces induced by the tensile forces of the stay cables. The applied compressive force amplifies the flexural behavior of girder and mast, which results in a beam-column effect. As the third factor, the large displacement or deformation effect produced by geometric change of the structure leads to geometric nonlinear behavior. Furthermore, the girder-mast-cable interaction affects the complex nonlinear behavior. When external load is applied to the girder first, it is transferred to the mast by stayed cables, because these connect the girder and mast. Because of the connection between the main members, the local structural behavior of each member affects the behavior of other members, which may result in global behavior and global changes of structural state. Finally, material nonlinearity may affect the structural behavior of cable-stayed bridges.

Studies to investigate the characteristics of structural stability or ultimate behavior of completed cable-stayed bridges have been performed. Researches have been performed to investigate the structural stability of completed cable-stayed bridges using eigenvalue analysis (Tang et al. 2001; Shu

✉ Young-Jong Kang
yjkang@korea.ac.kr

Seungjun Kim
skim@dju.kr

[1] Department of Construction Safety and Disaster Prevention Engineering, Daejeon University, Daejeon, South Korea

[2] Coastal Disaster Prevention Research Center, Korea Institute of Ocean Science and Technology, Busan, South Korea

[3] School of Architectural, Civil and Environmental Engineering, Korea University, Seoul, South Korea

and Wang 2001). In these studies, various buckling modes were introduced, and the effects of various geometric properties on the structural stability were described. But various nonlinearity factors were not considered in these studies, because they were conducted by conventional eigenvalue analyses. Furthermore, the initial condition, which can be considered by initial shape analysis, was not considered before considering the live load condition. This is very important, because cable-stayed bridges are designed with optimal initial tensile forces of cables, which make for minimum deformation and internal forces under dead load condition (Chen et al. 2000; Cheng and Xiao 2004; Kim and Lee 2001; Wang et al. 1993; Wang and Yang 1996).

It is well known that stability analysis or ultimate analysis of cable-stayed bridges should be conducted by nonlinear analysis due to various geometric and material nonlinearities and design characteristics of the structures (Adeli and Zhang 1995; Wang and Yang 1996; Xi and Kuang 1999; Ren 1999; Freire et al. 2006; Kim et al. 2015; Kim et al. 2016a, 2017). Ren (1999) studied the ultimate behavior of completed cable-stayed bridges considering various nonlinearities, boundary conditions, and loading conditions. Song and Kim (2007) also conducted nonlinear analysis for studying the ultimate capacity of cable-stayed bridges, and suggested an ultimate analysis method considering geometric and material nonlinearities. Kim et al. (2016a, b) conducted parametric study to investigate the effects of various design factors on the ultimate behavior of the cable-stayed bridges. The studies focuses on the ultimate capacity of completed cable-stayed bridges.

It is also well known that cable-stayed bridges under construction are more structurally unstable than the completed structure, because of the general construction method for the structures. As shown in Fig. 1, cable-stayed bridges during the construction stage have more unstable boundary conditions than the completed structure. After completing the construction, through the erection of the key segment of the girder, each part of the cable-stayed bridge is connected with each other part, so they are closed and they share the boundary conditions. But, before the closing and connection of two parts constructed individually, each part is supported by more unstable boundary conditions than the completed structure. Therefore, the ultimate behavior of each stage of construction should be analyzed and considered (Kim et al. 2017). Several researchers have studied the rational methodologies of construction stage analysis for cable-stayed bridges and suspension bridges (Reddy et al. 1999; Wang et al. 2004). The studies are limited to the general structural behavior of the cable-stayed bridge under construction, such as the characteristics of internal force distributions, structural deformations and so on. But the structural stability or ultimate behavioral characteristics of cable-stayed bridges during the construction stage has not been studied. Recently, Lee et al. (2015) experimentally studied the ultimate behavior of cable-stayed bridges under construction, and Kim et al. (2017) analytically studied the structural stability of cable-stayed bridges under construction by performing construction stage analysis based on geometric nonlinear analysis. In summary, the ultimate behavior of cable-stayed bridges under construction has not been actively studied.

In this analytical study, the ultimate behavior of steel cable-stayed bridges under construction is investigated. To perform rational ultimate analysis, a nonlinear analysis program for steel cable-stayed bridges is first developed, based on the theory of nonlinear finite element analysis. A three-step analysis method is suggested, in order to consider the characteristics of the design and construction method of cable-stayed bridges. Using this program, extensive analytical study is performed to investigate the ultimate behavior of steel cable-stayed bridges under construction, especially for the construction stage before the connection of two individual parts, because this stage might be considered as the most unstable state. By this analytical study, the governing factors affecting the ultimate behavior are classified. Furthermore, the effects of geometric properties, such as the cable-arrangement types, girder-mast flexural stiffness parameter and sectional area of stay cables, on the ultimate behavior and change of the ultimate mode and load carrying capacity are studied.

2 Theoretical Background

In this chapter, the theoretical background of ultimate analysis for steel cable-stayed bridges under construction is briefly introduced. Firstly, finite elements to model the main members of cable-stayed bridges are described, and the method to consider material nonlinearity of steel members is introduced. Secondly, a numerical strategy for incremental-iterative analysis is described. Finally, the analysis scheme of three-step ultimate analysis for steel cable-stayed bridges is proposed.

2.1 Finite Elements, Material Nonlinearity Consideration and Incremental-Iterative Analysis Strategy

2.1.1 Geometric and Material Nonlinearity Consideration

It is well known that cable-stayed bridges show various geometric nonlinearities, such as the cable-sag effect, beam-column effect of the girder and mast, large-displacement effect and girder-mast-cable interaction. So, nonlinear finite elements should be used to model the main members, because of those various nonlinearities.

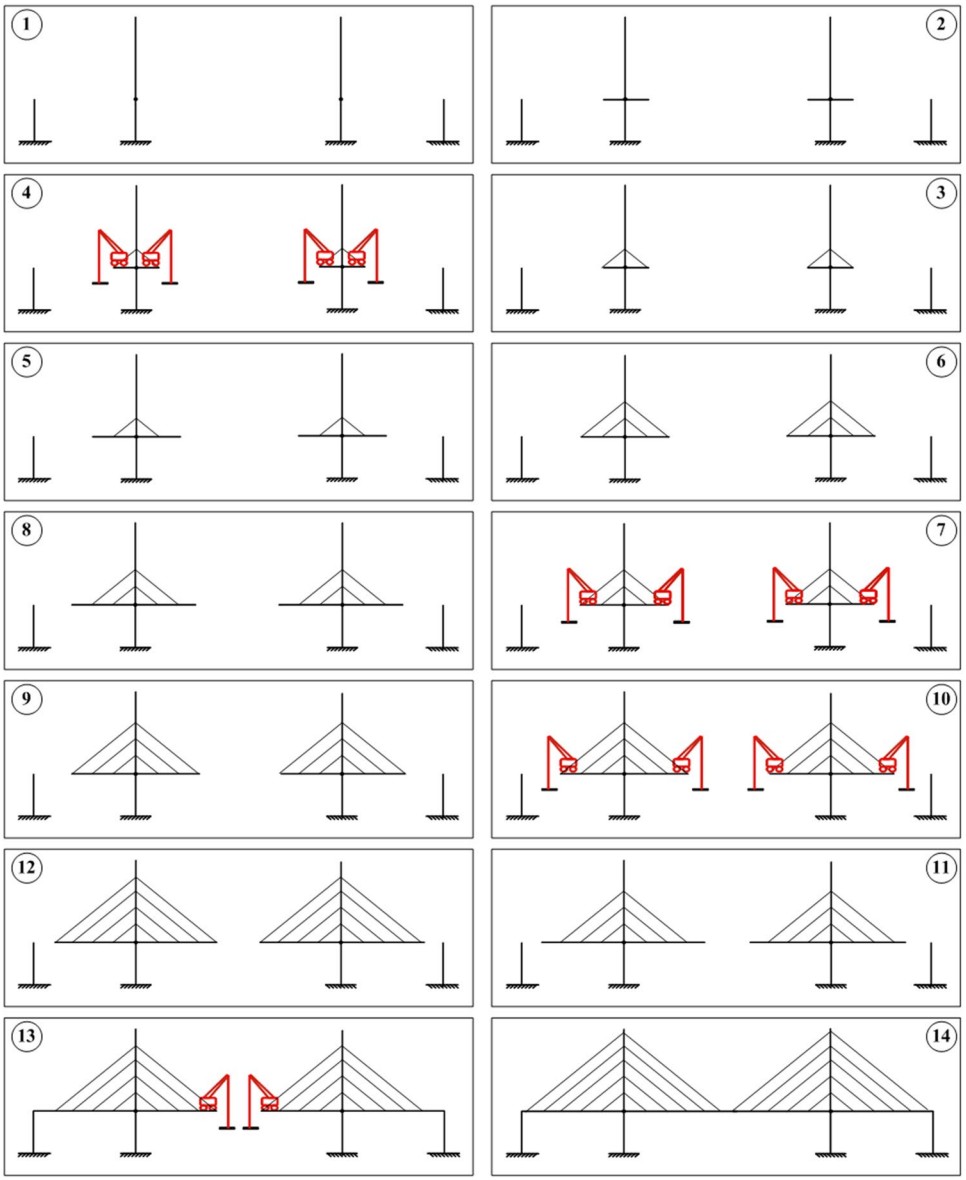

Fig. 1 General construction procedure for cable-stayed bridges (Kim et al. 2017)

To model the girder and mast, considered as the beam-column members, a nonlinear frame element that has 2 nodes and 6 degrees of freedoms is used. The element was derived based on the updated-Lagrangian formulation and the local stiffness matrix of this element, which consists of the elastic, geometric and induced matrices (Yang and Kuo 1994; Kim 2009; Kim et al. 2015; Kim and Kang 2016; Kim et al. 2016a, 2017). Figure 2 shows the nodal displacements and forces of the nonlinear frame element used in this study, and the Eqs. (1)–(3) describe the stiffness matrix composed of elastic, geometric and induced stiffness matrix (Yang and Kuo 1994; Lim et al. 2008; Kim and Kang 2016; Kim et al. 2015, 2016a, 2017).

$$[k] = [k_e] + [k_g] + [k_i] \tag{1}$$

where $[k_e]$ = elastic stiffness matrix; $[k_g]$ = geometric stiffness matrix; $[k_i]$ = induced stiffness matrix

$$[k_g] = \begin{bmatrix} a & 0 & 0 & 0 & -d & -e & -a & 0 & 0 & 0 & -n & -o \\ & b & 0 & d & g & k & 0 & -b & 0 & n & -g & k \\ & & c & e & -h & g & 0 & 0 & -c & o & -h & -g \\ & & & f & i & l & 0 & -d & -e & -f & -i & -l \\ & & & & j & 0 & d & -g & h & -i & p & -q \\ & & & & & m & e & -k & -g & -l & q & r \\ & & & & & & a & 0 & 0 & 0 & n & o \\ & & & & & & & b & 0 & -n & g & -k \\ & & & & & & & & c & -o & h & g \\ & & & & & & & & & f & i & l \\ & & & & & & & & & & j & 0 \\ & & & & & & & & & & & m \end{bmatrix} \tag{2}$$

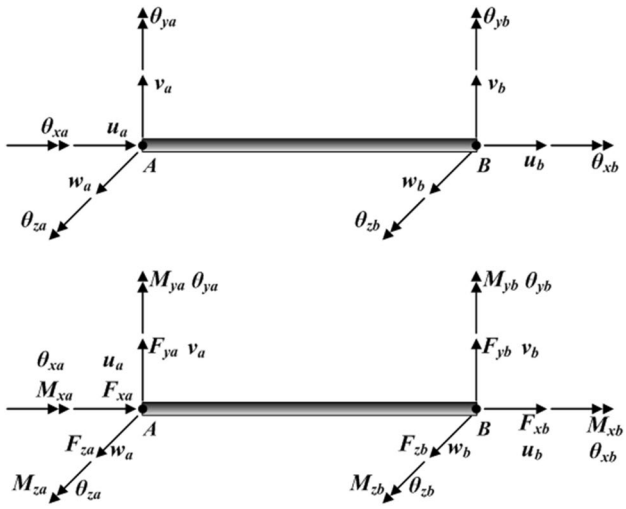

Fig. 2 Nodal displacements and forces of the nonlinear frame element

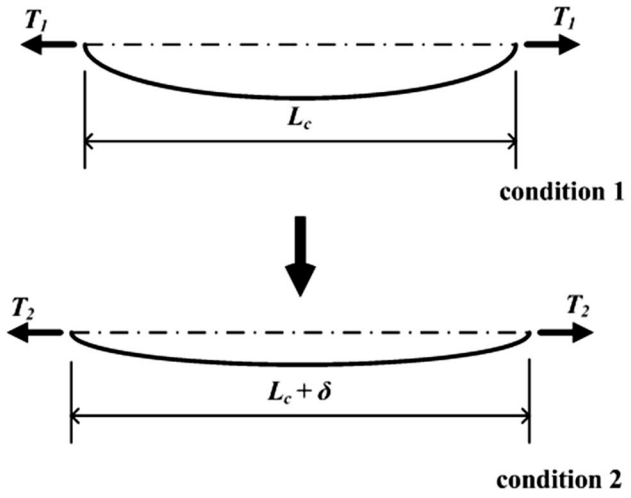

Fig. 3 Two conditions for a horizontal stay cable with tensile forces T_1 and T_2, respectively (Gimsing 1983; Kim and Kang 2016; Kim et al. 2015, 2016a, 2017)

where

$$a = \frac{{}^1F_{xb}}{{}^1L}, \quad b = \frac{6{}^1F_{xb}}{5{}^1L} + \frac{12{}^1F_{xb}I_z}{A{}^1L^3}, \quad c = \frac{6{}^1F_{xb}}{{}^1L} + \frac{12{}^1F_{xb}I_y}{A{}^1L^3},$$
$$d = \frac{{}^1M_{ya}}{{}^1L}, \quad e = \frac{{}^1M_{za}}{{}^1L},$$
$$f = \frac{{}^1F_{xb}J}{A{}^1L}, \quad g = \frac{{}^1M_{xb}}{{}^1L}, \quad h = \frac{{}^1F_{xb}}{10} + \frac{6{}^1F_{xb}I_y}{A{}^1L^2},$$
$$i = \frac{{}^1M_{za} + {}^1M_{zb}}{6}, \quad j = \frac{2{}^1F_{xb}{}^1L}{15} + \frac{4{}^1F_{xb}I_y}{A{}^1L},$$
$$k = \frac{{}^1F_{xb}}{10} + \frac{6{}^1F_{xb}I_z}{A{}^1L^2}, \quad l = -\frac{{}^1M_{ya} + {}^1M_{yb}}{6}, \quad m = \frac{2{}^1F_{xb}{}^1L}{15} + \frac{4{}^1F_{xb}I_z}{A{}^1L},$$
$$n = \frac{{}^1M_{yb}}{{}^1L}, \quad o = \frac{{}^1M_{zb}}{{}^1L},$$
$$p = \frac{{}^1F_{xb}{}^1L}{30} + \frac{2{}^1F_{xb}I_y}{A{}^1L}, \quad q = -\frac{{}^1M_{xb}}{2}, \quad r = -\frac{{}^1F_{xb}{}^1L}{30} + \frac{2{}^1F_{xb}I_z}{A{}^1L}$$

A = sectional area of the frame element; L = length of the frame element; I_y, I_z = 2nd moment of inertia with respect to the y and z axis, respectively; J = torsional constant

$$[k_i] = \begin{bmatrix} [0] & & & \\ & [k_i]_a & & \\ & & [0] & \\ & & & [k_i]_b \end{bmatrix} \tag{3}$$

where

$$[k_i]_a = \begin{bmatrix} 0 & 0 & 0 \\ {}^1M_{za} & 0 & -{}^1M_{xa}/2 \\ -{}^1M_{ya}/2 & {}^1M_{xa}/2 & 0 \end{bmatrix}$$

$$[k_i]_b = \begin{bmatrix} 0 & 0 & 0 \\ {}^1M_{zb} & 0 & -{}^1M_{xb}/2 \\ -{}^1M_{yb}/2 & {}^1M_{xb}/2 & 0 \end{bmatrix}$$

In the Eqs. (1)–(3), left superscript refers to the occurring configurations as below: 0 = initial undeformed configuration, 1 = last known deformed configuration, 2 = current deformed configuration. The terms without any superscript such as elastic modulus E are those at

the initial undeformed configuration. Also, every terms with superscript 1 are those at the current configuration, so they are updated at every incremental-iterative steps in order to obtain the physical terms at the current deformed configuration.

To model the cable member of cable-stayed bridges, a nonlinear equivalent truss element is used as shown in Figs. 3 and 4. This element was developed based on a nonlinear truss element with an equivalent modulus derived to consider the sag effect of the stay cables. The stiffness matrix of the element consists of the elastic stiffness and geometric stiffness, but the elastic modulus in the elastic stiffness is replaced by the equivalent modulus derived based on the force–elongation relationship of the elastic catenary (Ernst 1965; Fleming 1979; Gimsing 1983). In general, the conventional equivalent modulus of the common equivalent truss element was derived, with some simplification, by Taylor's series. But, in this study, the equivalent modulus of the force–elongation relationship of the elastic catenary, derived without any simplification, was used (Song et al. 2006; Kim 2009; Kim and Kang 2016; Kim et al. 2015, 2016a, 2017).

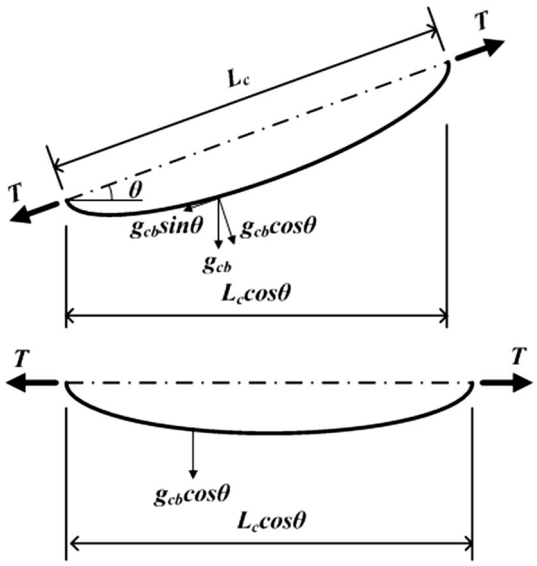

Fig. 4 Inclined stay cable and equivalent horizontal stay cable with equal deformational characteristics. g_{cb}: weight per unit length of a cable, T: tensile force (Gimsing 1983; Kim and Kang 2016; Kim et al. 2015, 2016a, 2017)

$$[k] = [k_e] + [k_g] = \frac{{}^1E_{eq} + {}^1A}{{}^1L_c}\begin{bmatrix} 1 & 0 & 0 & -1 & 0 & 0 \\ & 0 & 0 & 0 & 0 & 0 \\ & & 0 & 0 & 0 & 0 \\ & & & 1 & 0 & 0 \\ & & & & 0 & 0 \\ & & & & & 0 \end{bmatrix} + \frac{{}^1\tau_{11}{}^1A}{{}^1L_c}\begin{bmatrix} 1 & 0 & 0 & -1 & 0 & 0 \\ & 1 & 0 & 0 & -1 & 0 \\ & & 1 & 0 & 0 & -1 \\ & & & 1 & 0 & 0 \\ & & & & 1 & 0 \\ & & & & & 1 \end{bmatrix} \tag{4}$$

where $[k]$ = stiffness matrix of a nonlinear equivalent truss element; $[k_e]$ = elastic stiffness matrix; $[k_g]$ = geometric stiffness matrix; ${}^1E_{eq} = {}^1E_{\tan}$ or ${}^1E_{\sec}$; ${}^1E_{\tan}$ = tangential modulus; ${}^1E_{\sec}$ = secant modulus; ${}^1\tau_{11}$ = axial stress of a cable member;

$$E_{\tan} = \frac{E}{\left(1 + K_1 + K_2\right)/2\cosh\left(\frac{g_{cb}L_c\cos\theta}{2T_i}\right)} \tag{5}$$

where

$$K_1 = \frac{1}{g_{cb}\cdot L_c\cos\theta}\left[2T_i\sinh\left(\frac{g_{cb}\cdot L_c\cos\theta}{T_i}\right) - g_{cb}\cdot L_c\cos\theta\cdot\sinh\left(\frac{g_{cb}\cdot L_c\cos\theta}{T_i}\right)\right]$$

$$K_2 = \frac{-4EA}{g_{cb}\cdot L_c\cos\theta}\left[\sinh\left(\frac{g_{cb}\cdot L_c\cos\theta}{2T_i}\right) - \frac{g_{cb}\cdot L_c\cos\theta}{2T_i}\cdot\cosh\left(\frac{g_{cb}\cdot L_c\cos\theta}{2T_i}\right)\right]$$

${}^1A$ = sectional area of a cable member; ${}^1L_c$ = length of a cable members

$$E_{\sec} = \frac{\left(T_f - T_i\right)}{\frac{\delta}{c}} = \frac{E}{\left(1 + K_1 + K_2\right)/2\cosh\left(\frac{g_{cb}\cdot L_c\cos\theta}{2T_f}\right)} \tag{6}$$

where

$$K_1 = \frac{1}{g_{cb} \cdot L_c \cos\theta \left(T_f - T_i\right)} \left[T_f^2 \sinh\left(\frac{g_{cb} \cdot L_c \cos\theta}{T_f} \right) - T_i^2 \sinh\left(\frac{g_{cb} \cdot L_c \cos\theta}{T_i} \right) \right]$$

$$K_2 = \frac{4EA}{g_{cb} \cdot L_c \cos\theta \left(T_f - T_i\right)} \left[T_i \sinh\left(\frac{g_{cb} \cdot L_c \cos\theta}{2T_i} \right) - T_f \sinh\left(\frac{g_{cb} \cdot L_c \cos\theta}{2T_f} \right) \right]$$

g_{cb} = weight per unit length of the cable; T_i = tensile force at condition 1; T_f = tensile force at condition 2; $L_c \cos\theta$ = horizontally projected length of the cable.

To consider the material nonlinearities of steel members modeled by line elements, several methods can be used, such as the plastic zone method, plastic hinge method and refined plastic hinge method. Among these methods, the plastic zone method guarantees the best numerical accuracy. But it requires substantial calculation efforts. So, in this study the refined plastic hinge method is adopted and used, because of its efficiency and accuracy. The refined plastic hinge method uses the tangential modulus E_t to consider the effect of the gradual yield by axial force, and the scalar parameter η to consider the effect of the gradual yield and plastic hinge occurrence by applied axial force and bending moment (Liew et al. 1993; Song and Kim 2007; Kim 2009; Kim et al. 2016a, 2017). Using the tangential modulus and scalar parameter, the elastic stiffness matrices of the nonlinear frame element and nonlinear equivalent truss element are modified.

2.1.2 Numerical Solution Strategy for Nonlinear Finite Element Analysis

As the numerical strategy of the incremental-iterative analysis method for nonlinear analysis, there are several numerical methods, such as the Newton–Rapshon method, arc-length method, work control method and generalized displacement control method. Because cable-stayed bridges have various geometric and material nonlinearities, complex nonlinear responses may occur when the structure is subjected to external forces. The numerical methods can be classified into several categories, such as the force-control method, displacement-control method, and work control method. In general, a force-control method, such as the Newton–Rapshon method, is not appropriate for tracing complex nonlinear response. For the response, a displacement or work control method is widely used. Among these methods, the arc-length method (Crisfield 1983) has been widely used. But there is a problem in the constraint equation of the method, in that the units of each term are not the same, and this inequality of units may induce numerical instability when the structural response reaches towards ultimate state (Yang and Kuo 1994). So, the generalized displacement control method (Yang and Kuo 1994) is used in this study. Using this method, the incremental-iterative load factors are calculated and applied during nonlinear analysis, so that the complex nonlinear response of cable-stayed bridges can be traced with numerical stability.

$$\lambda_1 = \pm \lambda_1^1 |GSP|^{1/2} \quad (j = 1) \tag{7}$$

$$\lambda_j = -\frac{\left\{\Delta \hat{U}_1^{i-1}\right\}^T \left\{\Delta \bar{U}_j\right\}}{\left\{\Delta \hat{U}_1^{i-1}\right\}^T \left\{\Delta \hat{U}_j\right\}} \quad (j \geq 2) \tag{8}$$

where $GSP = \frac{\left\{\Delta \hat{U}_1^1\right\}^T \left\{\Delta \hat{U}_1^1\right\}}{\left\{\Delta \hat{U}_1^{i-1}\right\}^T \left\{\Delta \hat{U}_1\right\}}$, generalized stiffness parameter; λ_j^i = ith incremental, jth iterative analysis load factor; λ_1^1 = preset load increment factor; $\{\Delta \bar{U}\}$ = incremental displacement vector by unbalanced force vector; $\{\Delta \hat{U}\}$ = incremental displacement vector by total load vector.

2.2 Analysis Strategy of the Ultimate Analysis for Steel Cable-Stayed Bridges

The ultimate behavior of steel cable-stayed bridges under construction is analyzed by a three-step analysis scheme, as shown in Fig. 5, in order to rationally consider the characteristics of the design and construction method of cable-stayed bridges. Firstly, initial shape analysis (Fig. 6) is performed to determine optimal tensile forces of the stay cables, which ensure that the structure suffers minimal deformation under the dead load condition, and to reflect the structural state before live load analysis. Secondly, construction stage analysis using the backward process analysis method (Fig. 7) is performed to research the structural state under construction. After that, external load analysis is performed to trace the nonlinear response, and to find the ultimate behavior under specific external load condition. All three analyses, initial shape analysis, construction stage analysis and live load analysis, are performed based on the theory of nonlinear finite element analysis; thus geometric and material

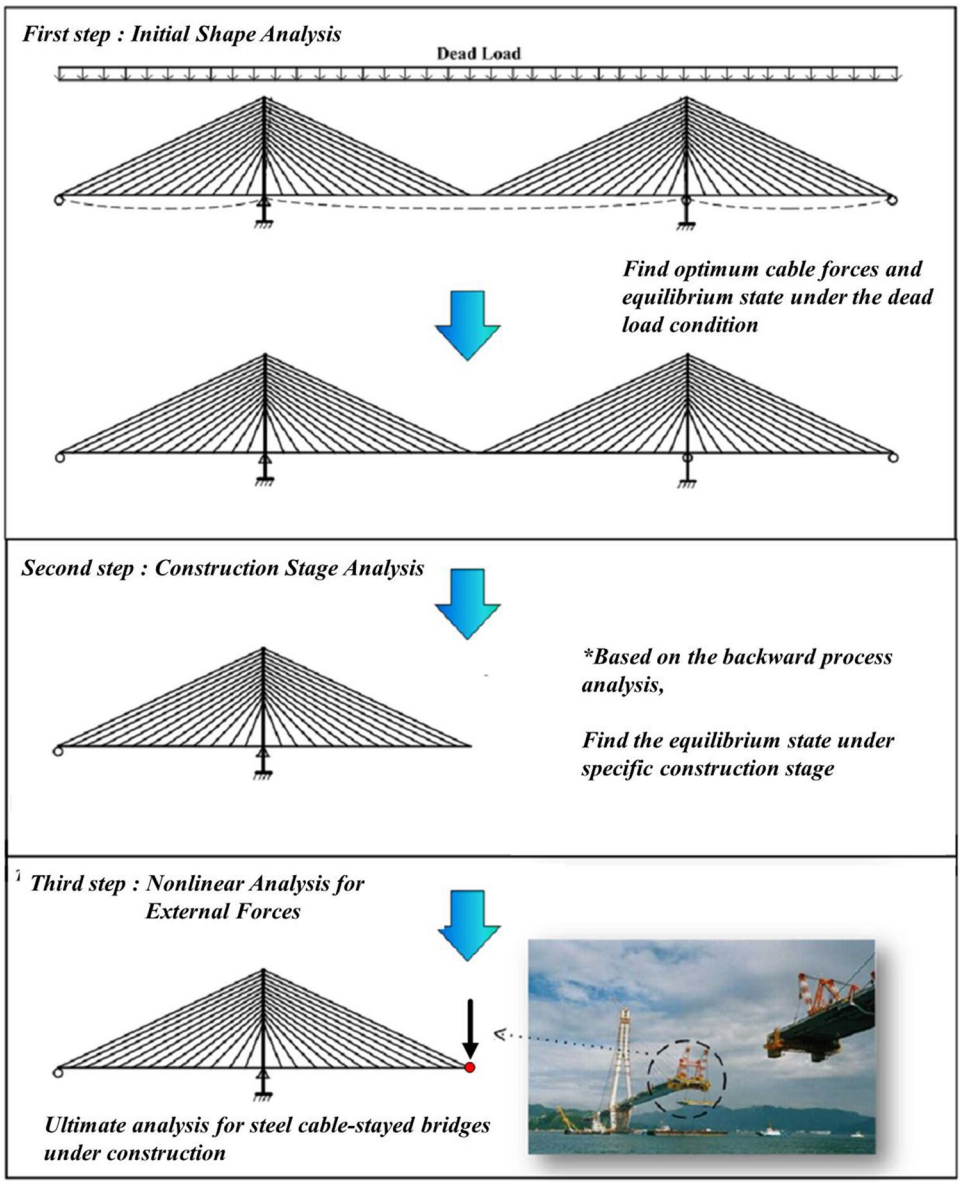

Fig. 5 Analysis strategy of ultimate analysis for steel cable-stayed bridges under construction

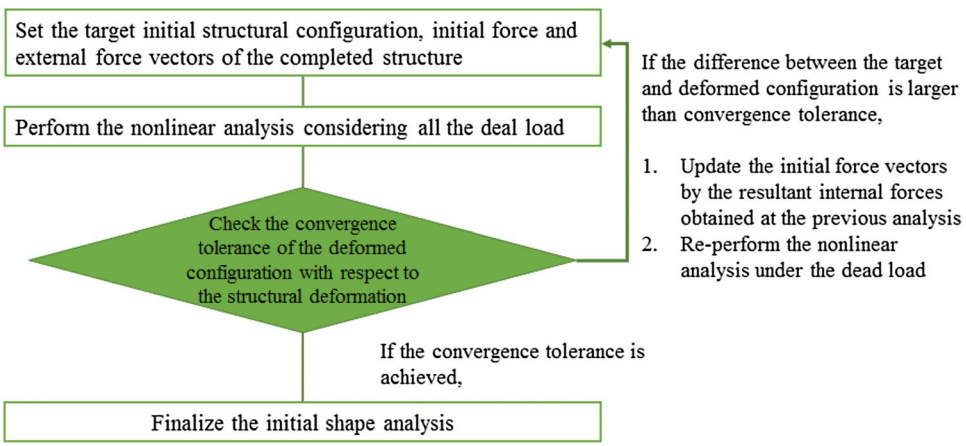

Fig. 6 Procedure of initial shape analysis (Kim et al. 2017)

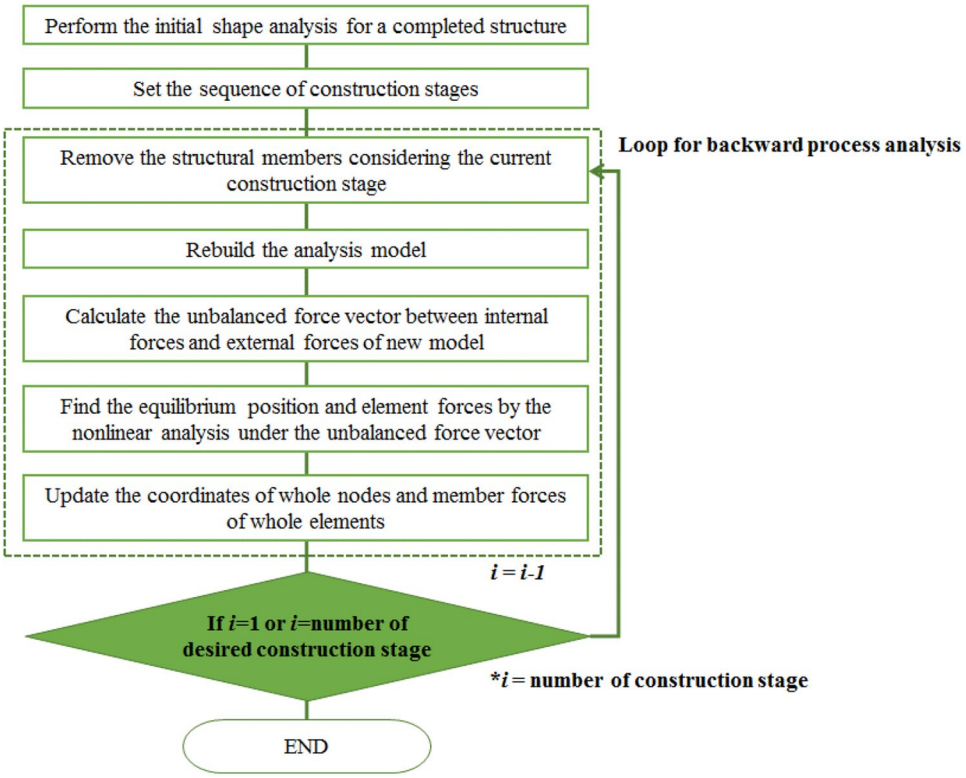

Fig. 7 Backward process method for the construction stage analysis (Kim et al. 2017)

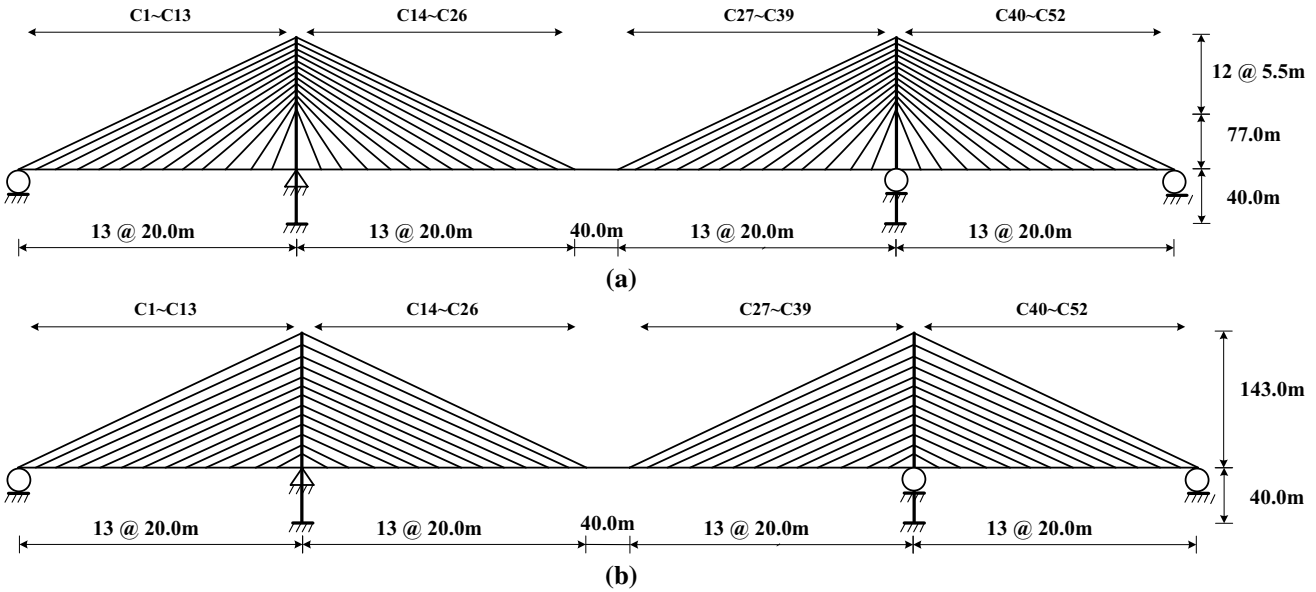

Fig. 8 Completed analysis model. **a** Fan type model. **b** Harp type model

nonlinearities of steel cable-stayed bridges are considered during the structural analyses. The analysis program was written using Visual C++ V6.0. As well as the numerical modulus, a simple post processor is also made to intuitively observe the structural behavior.

Validation of the consideration method for the geometric and material nonlinearities, initial shape analysis and construction stage analysis methods were performed in former papers and researches (Yang and Kuo 1994; Song et al. 2006; Lim et al. 2008; Song and Kim 2007; Kim 2009; Kim

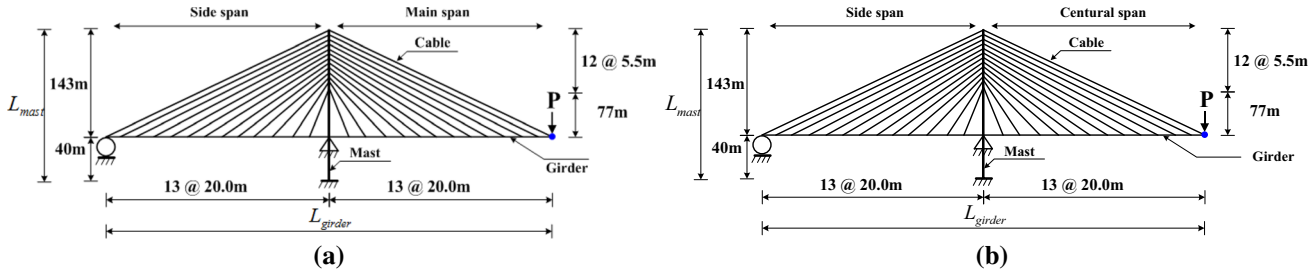

Fig. 9 Analytical model under construction stage. **a** Fan type model. **b** Harp type model

Fig. 10 Section of the girder

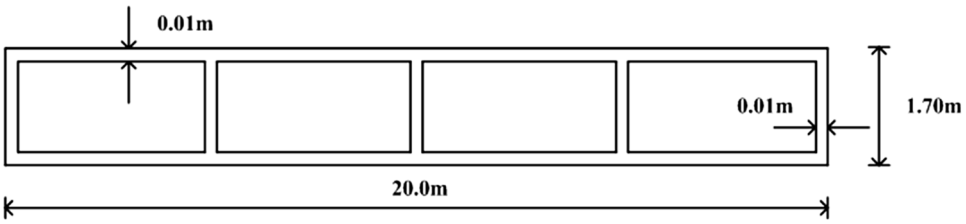

Table 1 Material and geometric properties of main members

	Girder	Mast	Cable
E (kN/m^2)	2.1×10^8	2.1×10^8	2.1×10^8
A (m^2)	0.484	0.214–1.006	0.01–0.12
I (m^4)	0.305	0.214–10.719	–
γ (kN/m^3)	157.74	78.0	78.0

Table 2 Considered girder-mast flexural stiffness ratio

	Fan type	Harp type
$\frac{E_m I_m/L_m}{E_g I_g/L_g}$	2.00–30.00	2.00–30.00

E_m: Elastic modulus of a mast, E_g: Elastic modulus of a girder, I_m: 2nd Moment of inertia of a mast, I_g: 2nd Moment of inertia of a girder, L_m: Length (Height) of the mast, L_g: Length of the girder

et al. 2017). So, detailed descriptions of the validations are omitted in this paper.

3 Ultimate Behavior of Steel Cable-Stayed Bridges Under Construction

3.1 Analysis Model

Figures 8 and 9 show analysis models considered in this study. The models are basically divided into two different cable-arrangement types, the fan type model and harp type model. The completed structure models shown in Fig. 8 are firstly analyzed by initial shape analysis, and then construction stage analysis is performed to find the structural equilibrium state of the construction stage model, as shown in Fig. 9. Finally, nonlinear analysis for the ultimate behavior

Fig. 11 Loading/boundary condition of the examined models

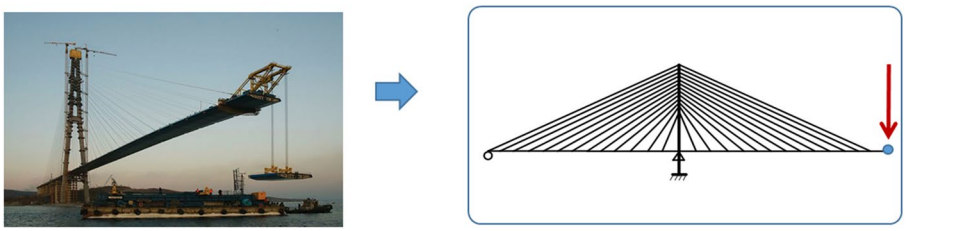

under the external load condition is performed. Figure 10 shows the section of the girder. The section of the mast is considered as a box section of various sectional sizes, to investigate the effect of mast stiffness. It is assumed that there are sufficient stiffeners to prevent local buckling in the section of the girder and mast. Finally, a circular section is considered as the section of the cable, and various areas are considered in order to investigate the effect on structural stability. Table 1 represents the material and geometric properties of girder, mast, and cables. In this study, girder-mast flexural stiffness ratio is considered as the main parameter, which mainly affects the characteristics of the ultimate behavior of the structure. Table 2 shows the range of girder-mast stiffness ratios considered in this study. Also, the sectional area of stay cables is considered as a variable, to investigate the effect on the ultimate behavior. After extensive parametric study, considering different cable-arrangement types, various girder-mast flexural stiffness ratios and sectional areas of stay cables, the governing factors that mainly affect the ultimate behavior are classified into two types. Also, the effects of girder-mast stiffness ratio and cable area on the change of ultimate behavior and ultimate load carrying capacity are investigated.

Figure 11 presents the loading and boundary condition. As shown in this figure, the analytical model that performed the construction stage analysis (using the backward process analysis method) is subjected to a concentrated load, that reflects the weight of a derrick crane and a key segment of the girder. Thus, the ultimate analysis for steel cable-stayed bridges under construction is performed by three-step analysis, namely initial shape analysis, backward process analysis, and external load analysis.

3.2 Ultimate Mode 1: Girder-Mast Interactive Buckling

As the first ultimate mode, girder-mast interactive buckling is introduced in this chapter. It can be supposed that if the

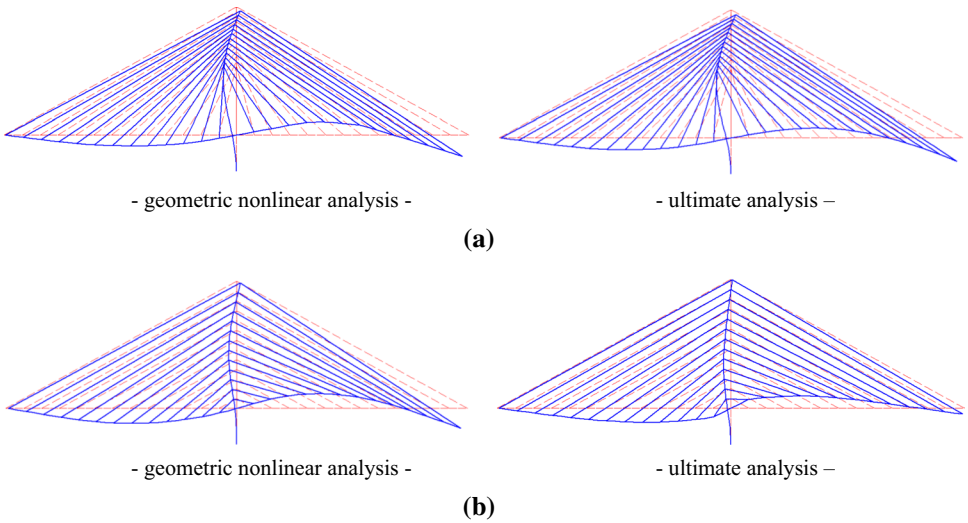

Fig. 12 Deformed shapes of analysis models which have a 2.0 girder-mast stiffness ratio. **a** Fan type model. **b** Harp type model

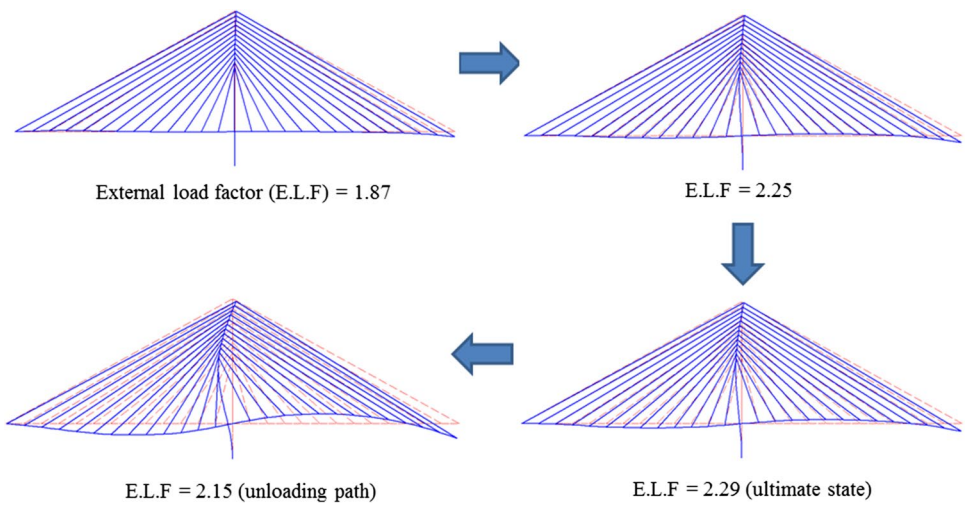

Fig. 13 Deformation sequence of the girder-mast interactive buckling. (Fan type model, girder-stiffness ratio = 2.0, $A_c = 0.02\ m^2$, scale factor = 2.0)

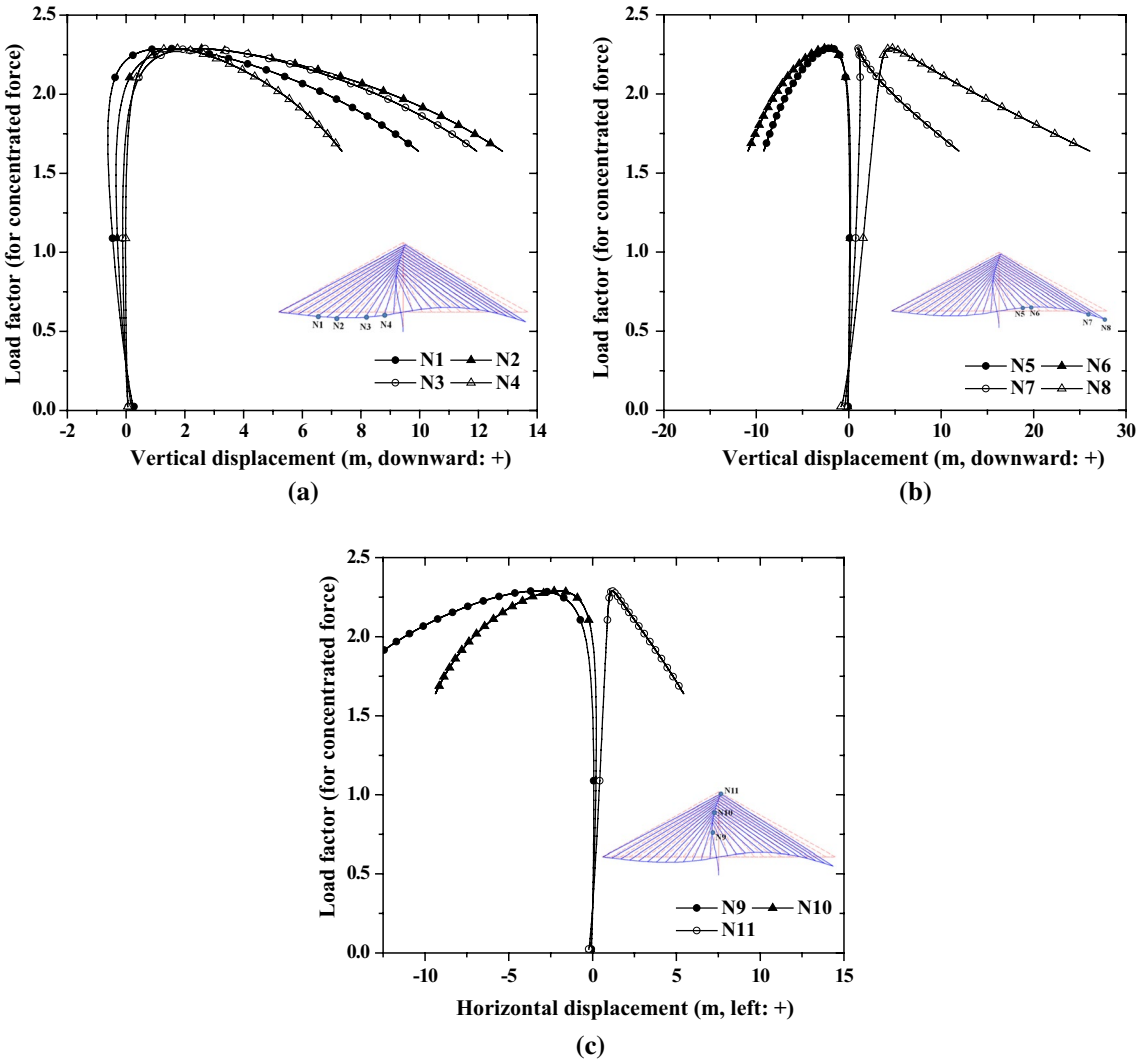

Fig. 14 Load-displacement curves of fan type model, girder-mast stiffness ratio: 2.0. **a** Points at the left side span girder. **b** Points at the center span girder. **c** Point at the mast

main members, girder and mast, don't have sufficient flexural stiffness, buckling may occur due to applied compressive force induced by stay cables. Figure 12 shows the girder-mast interaction buckling mode of steel cable-stayed bridges under construction.

In other words, when the girder-mast stiffness ratio is quite small, the mast can't resist the mast buckling, and girder and mast suffer significant flexural deformation when the external force applied to the tip of the center span increases. The flexural deformation is definitely induced by the beam-column effect of the girder and mast subjected to increasing compressive forces by stay cables. The structural behavior can be classified as buckling. Also, the deformations obtained by geometric nonlinear analysis and ultimate analysis (which means nonlinear analysis with considering both nonlinearities) are almost the same. So, it can be concluded that girder-mast interactive buckling governs the ultimate behavior of a structure that has relatively low flexural stiffness of the mast.

Figure 13 shows the sequence of structural deformation when girder-mast buckling governs the ultimate behavior. As shown in the figure, the flexural deformation of the girder and mast is amplified, because of the beam-column effect. When vertical force is applied to the tip of the center span, the center span deflects, and the deflection leads to horizontal movement of the mast. As the external force increases more and more, the deformation of the girder and mast increases, and the tensile forces of stay cables also continuously increase to resist the deformation. So, the compressive forces applied to the girder and mast increase, due to increase of the tensile forces of the stay cables. Finally, the beam-column effect is amplified because of the increasing

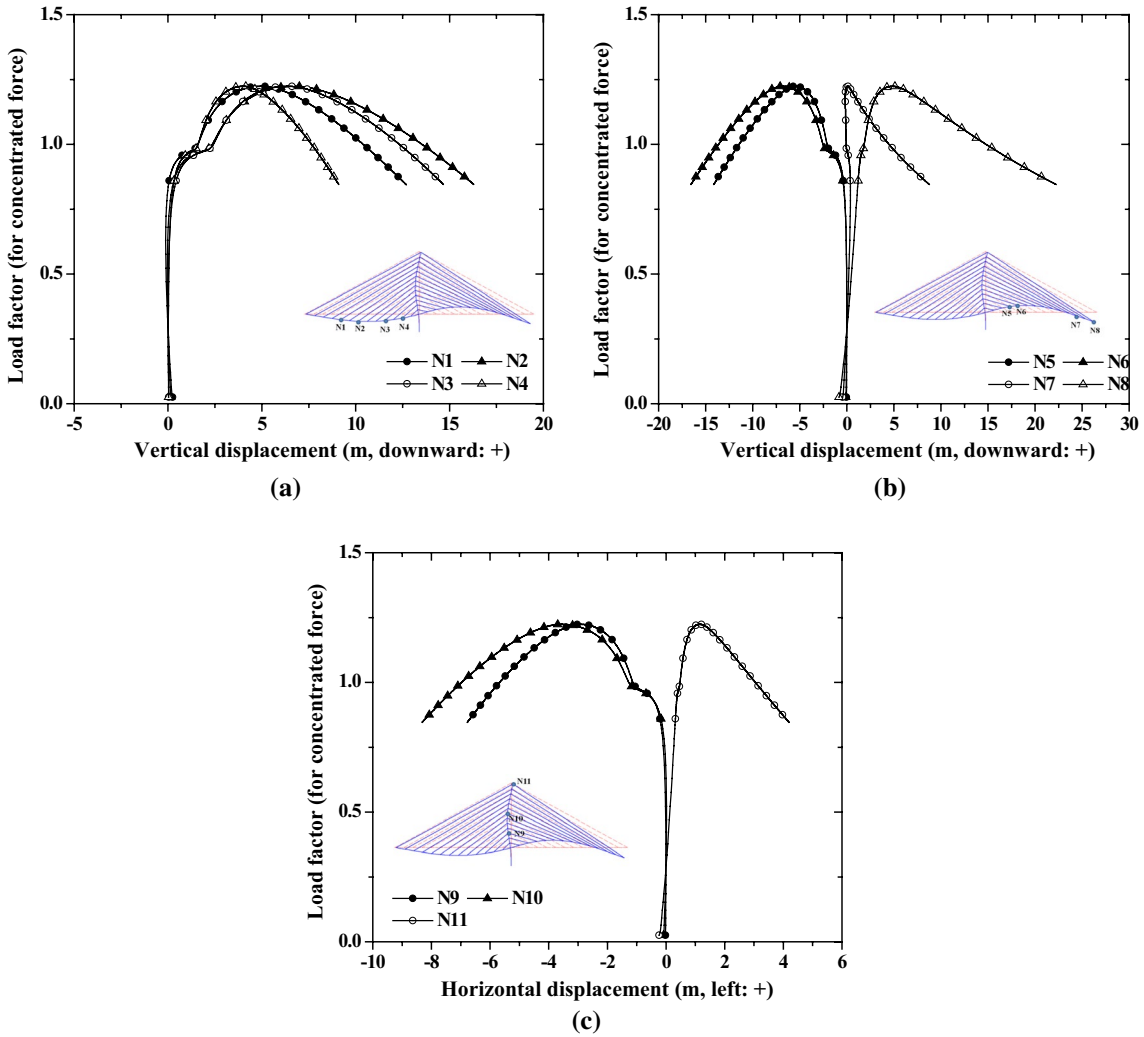

Fig. 15 Load-displacement curves of harp type model, girder-mast stiffness ratio: 2.0. **a** Points at the left side span girder. **b** Points at the center span girder. **c** Point at the mast

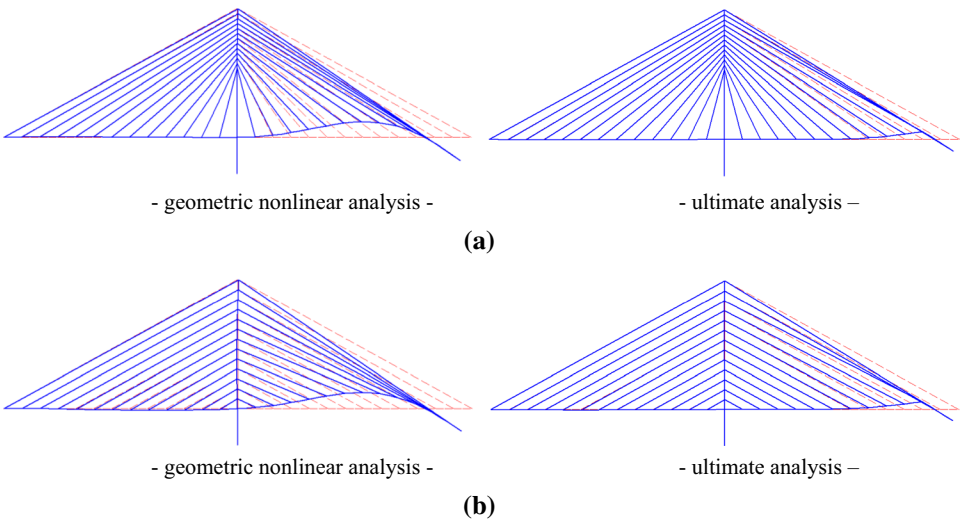

Fig. 16 Deformed shapes of analysis models which have a 30.0 girder-mast stiffness ratio. **a** Fan type model. **b** Harp type model

compressive forces, and the effect leads to buckling of the main members.

In Figs. 14 and 15, the load–displacement curves of the models show the girder-mast interactive buckling, obtained by ultimate analysis. As shown in the figures, there are significant ultimate load factors. Every point in the structure shows continuous deformation, although the external force decreases after the ultimate point. In other words, the structural deformation continuously grows while the external force decreases, because of the amplification of the deformation induced by the buckling.

3.3 Ultimate Mode 2: Material Yield of the Girder at the Center Span

According to the analysis result in this study, there is no significant flexural deformation of the mast in the models that have relatively high flexural stiffness of the mast. Instead, the center span shows the deformation. As shown in Fig. 16, it can be expected that the center span suffers negative flexural deformation, when the external force applied to the tip of the girder increases. The deformation is quite interesting, because the force is applied downward. If the center span behaves as a cantilever beam, the structure may show negative flexural deformation downward at all points. But, there is upward deformation while the external force is applied downward. This is basically caused by the beam-column effect. When the external force increases, the tensile forces of the cables that support the center span also increases, to resist the deflection of the span. So, the compressive forces applied to the girder increase, and produce the beam-column effect of the girder. Because of the effect, the center span suffers the deformation shown in Fig. 16. Incidentally, there are some different shapes between the deformations obtained by the two analysis methods. According to the result of ultimate analysis, plastic hinges occur near the tip of the center span, because of excessive bending moment with compressive force. Based on this fact with the difference of the deformations shown in the figure, it can be concluded that the material yield that occurs at the center span may govern the ultimate behavior of the models that are designed with sufficient flexural stiffness of the mast. As the external force increases, the flexural deformation of the center span grows, until some section reaches the material limitation, and the structure finally becomes the ultimate state.

Figure 17 shows the sequence of structural deformation when the material yield of the center span governs the ultimate behavior. When external force is applied to the tip of the center span, the tip of the center span starts to move downward, and the mast also moves horizontally, because of the downward movement of the span. Further, the horizontal movement of the mast makes for upward lifting of the side span. As the structural deformation grows and is amplified by the beam-column effect, a specific section in the center span finally reaches its material limitation, because of excessive internal forces. So the structure reaches the ultimate state, and the external force starts to decrease. As the external force decreases, the deformations of the mast and side span are recovered, and both main members move back to their original position.

Figures 18 and 19 indicate the load–displacement curves at the girder and mast. The curves show well the structural behavior of these models. As mentioned previously, the mast and side span move back to their original positions as the live load factor decreases. But the region near the plastic hinge at the center span suffers continuous deformation, whereas the live load decreases. Thus, it can concluded that material yield near the tip of the center span governs the ultimate behavior of the structure, when the flexural stiffness of the mast is sufficient to resist mast buckling.

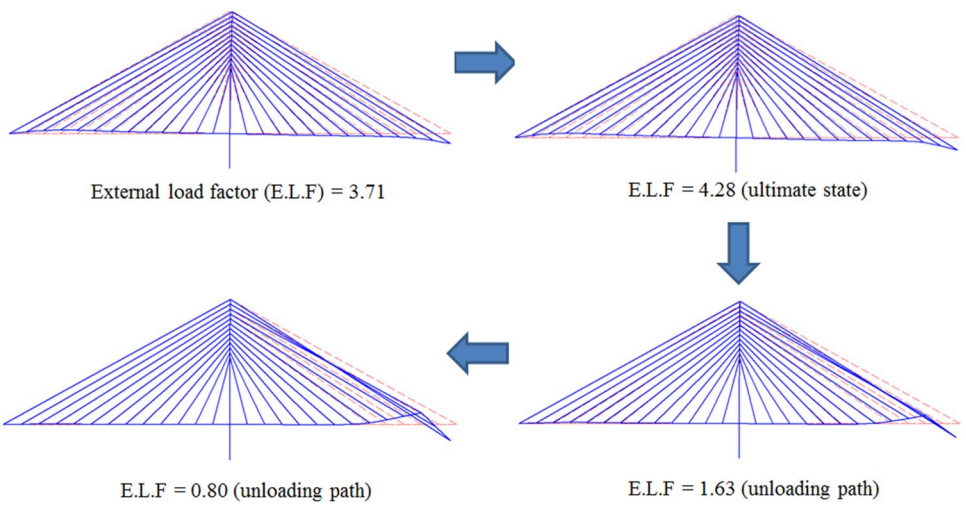

Fig. 17 Deformation sequence of material yield. (Fan type model, girder-stiffness ratio = 30.0, $A_c = 0.02\ m^2$, scale factor = 2.0)

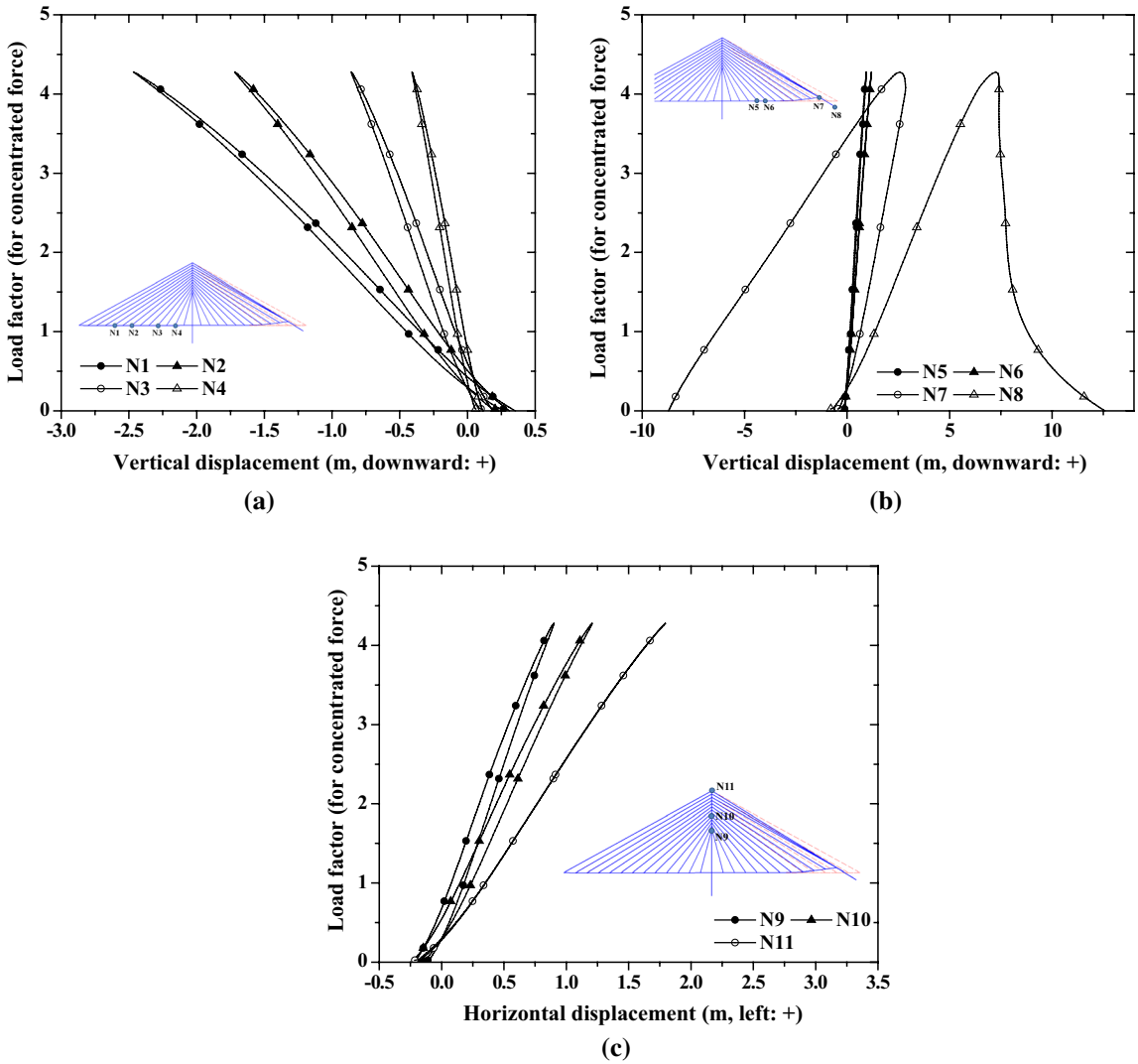

Fig. 18 Load-displacement curves of fan type model, girder-mast stiffness ratio: 30.0. **a** Points at the left side span girder. **b** Points at the center span girder. **c** Point at the mast

3.4 Effect of the Girder-Mast Stiffness Ratio on the Change of Ultimate Mode

As described previously, the ultimate mode varies with respect to the girder-mast stiffness ratio. If the ratio is quite small, girder-mast interactive buckling might govern the ultimate behavior. Also, if the ratio is large, material yield of the girder at the center span governs the ultimate behavior. In this chapter, the effect of the girder-mast stiffness ratio on the change of ultimate mode and load carrying capacity of the structure is described.

Figures 20 and 21 show the change of the ultimate mode shapes by the change of girder-mast stiffness ratio. As shown in those figures, the governing factor changes from girder-mast interactive buckling, to plastic hinge occurrence at the center span, as the ratio increases.

Figure 22 shows the change of the critical/ultimate live load factor with respect to the girder-mast stiffness ratio. To study the governing factors of the ultimate behavior more clearly, the ultimate live load factor is compared with the critical live load factor, which is obtained by geometric nonlinear analysis.

As shown in the figure, the governing mode for ultimate behavior can be classified into two modes, which are the girder-mast interactive buckling mode and the girder yield mode. In the girder-mast interactive buckling mode, both analysis results are almost the same, because the buckling is absolutely affected by the geometric nonlinearities. Whereas, there are significant differences between the load carrying capacities obtained by both analysis methods in the center span yield mode, because of the material limitation. As the stiffness of the mast increases, the governing mode

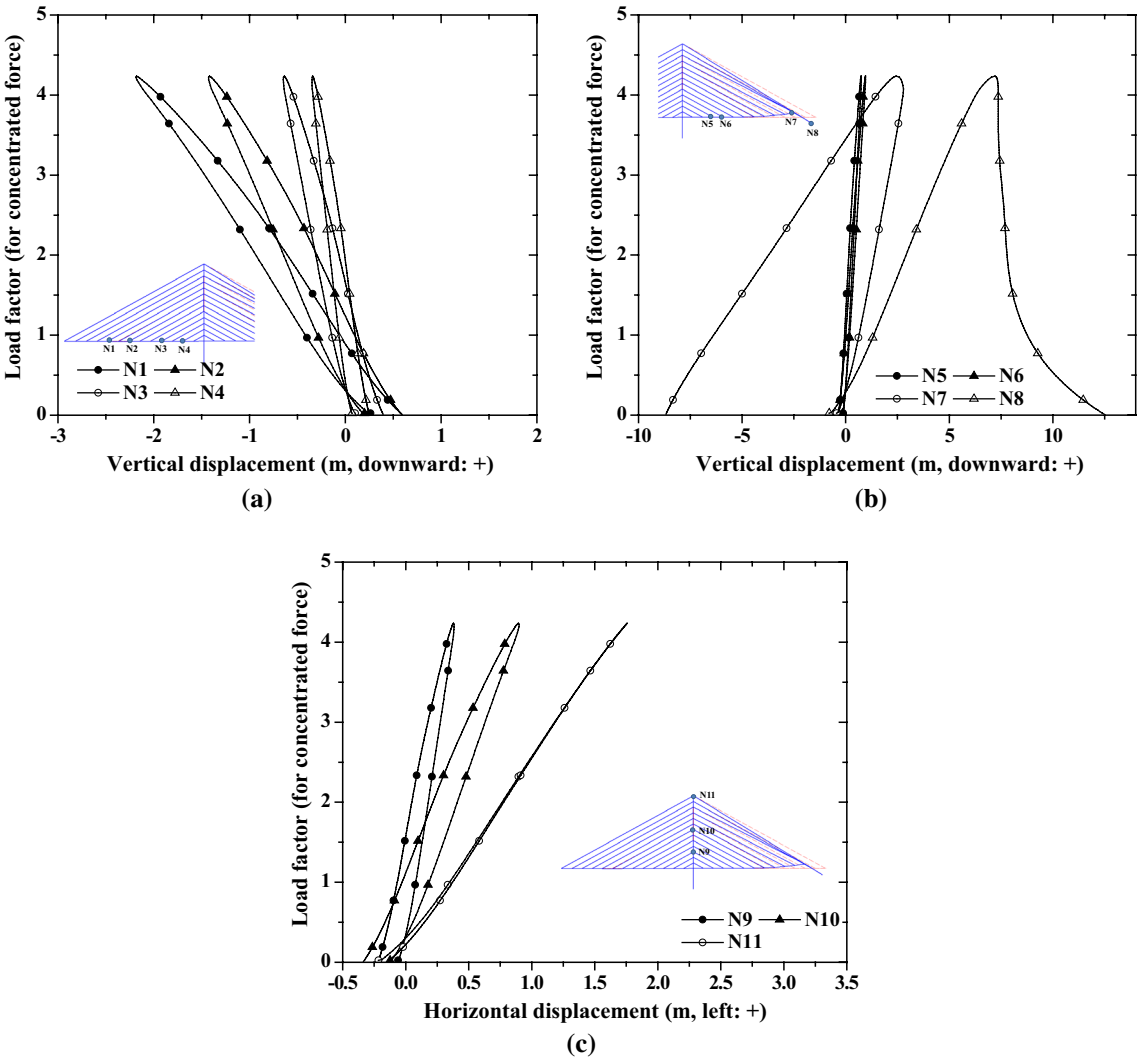

Fig. 19 Load-displacement curves of harp type model, girder-mast stiffness ratio: 30.0. **a** Points at the left side span girder. **b** Points at the center span girder. **c** Point at the mast

changes from buckling to material yield. For efficient use of material, buckling should be prevented. Also, the live load factors of both models converge to the specific load factor as the girder-mast stiffness ratio increases. After the governing factor changes from buckling to material yield, continuous increase of load carrying capacity does not occur, despite the stiffness of the mast increasing more and more. Consequently, these results indicate that there is a minimum required flexural stiffness of the mast to prevent girder-mast interactive buckling, and the stiffness can be a sufficient stiffness ratio for the structure before complete construction.

Figure 23 shows a comparison of the ultimate/critical load factors of the fan type and harp type models. In general, it can be supposed that the structure that has a higher cable arrangement angle will show a better structural efficiency under the vertical load condition. Based on force-equilibrium, more tensile forces are required at the lower stay cables, when the same vertical force components are required to resist the vertical deformation of the girder. Also, it produces larger compressive forces applied to the girder. As shown in the figure, the fan type model shows a higher ultimate/critical load factor than the harp type, because of that reason. Incidentally, the load carrying capacities of both models converge as the girder-mast stiffness ratio increases. In particular, if the girder-mast stiffness ratio is larger than 15.0, the load carrying capacities of each model become almost the same. This can be also explained with the load-cable force curve shown in the next figures.

As shown in Figs. 24 and 25, most cables lose their tensile forces as the external load increases. The loss of tensile forces of the stay cables is induced by the shortening of

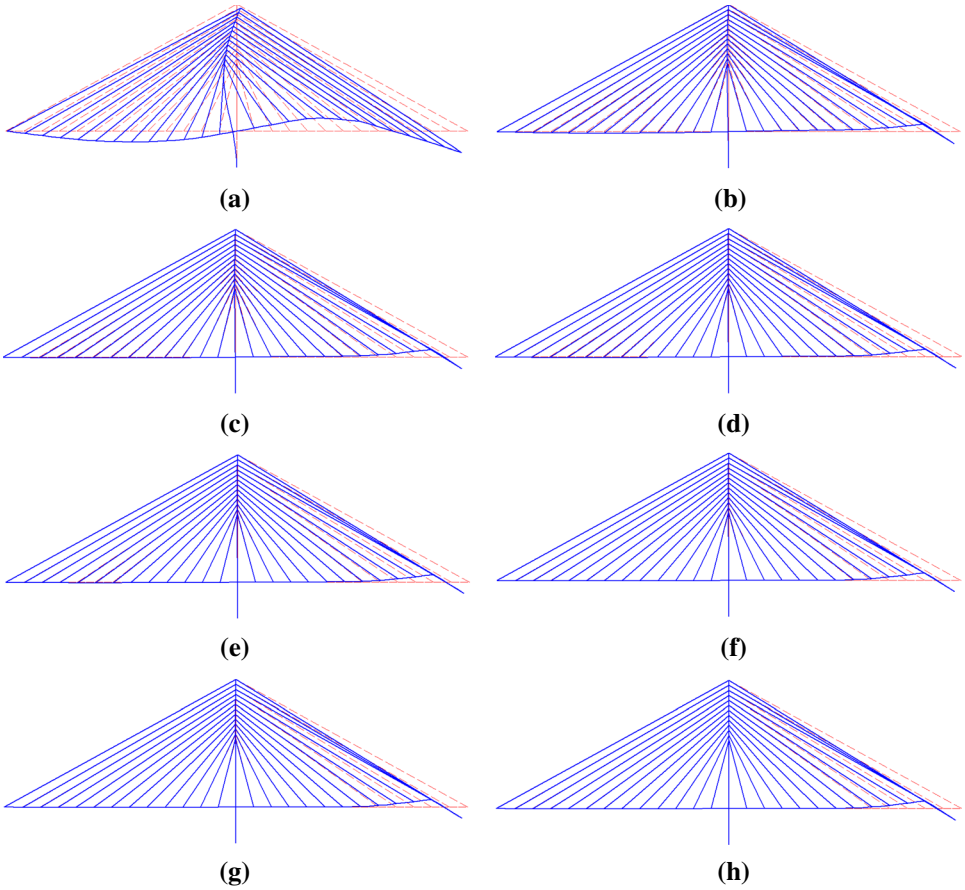

Fig. 20 Ultimate mode shape of fan type models. **a** Girder-mast flexural stiffness ratio: 2.0. **b** The stiffness ratio: 3.0. **c** The stiffness ratio: 5.0. **d** The stiffness ratio: 7.0. **e** The stiffness ratio: 9.0. **f** The stiffness ratio: 15.0. **g** The stiffness ratio: 20.0. **h** The stiffness ratio: 30.0

the relative distance between the center span and mast. The upward deformation of the center span induced by the beam-column effect produces the shortening. The loss of tensile force indicates the decrease of compressive force applied to the girder and mast. As most of the cables (except the exterior cables) of the center span lose their tensile force, only exterior cables, such as cables 25 and 26, apply compressive force to the girder and mast. Incidentally, the stay angles of exterior cables of the fan type model and harp type model are almost the same. This eventually means that the compressive forces applied to the center spans of both models converge. Thus, the ultimate load capacities also become almost the same under the same force condition.

3.5 Effect of the Sectional Area of Stay Cables

It can be simply supposed that the increase of sectional area of the stay cables induces an increase of the stiffness and strength of cable-stayed bridges. It is quite true that the increase of the sectional area induces elastic stiffness and strength of the axial member. Based on this simple theory, the assumption may be reasonable. To study the effect of the sectional area of stay cables, a parametric study was performed by considering various sectional areas of cables. Figure 26 shows the change of the ultimate load factor with respect to the sectional area of the stay cables.

In the girder-mast interactive buckling mode, an increase of sectional area of the stay cables produces a decrease of the ultimate load carrying capacity. There are positive and negative effects of the increase of sectional area of the stay cables. Firstly, the increase of sectional area makes for an increase of elastic stiffness of the axial members, which is a positive effect. But, the increase of the sectional area also makes for an increase of the sag effect, because of the increase of the own weight of the cables, which is an absolutely negative effect. Moreover, the compressive force applied to the mast also increases, because of the increase of the own weight of the cables, which is a second negative effect. Because the compressive force applied to the mast is very important in this ultimate mode, the ultimate load factor decreases as the sectional area increases, although a positive effect also exists.

In the girder yield mode, the curves show a peak point, which indicates the maximum ultimate load carrying capacity. The graph can be divided into two parts. The first part shows the increase of critical load factor as the cable area increases; it can be said that the increase of elastic stiffness

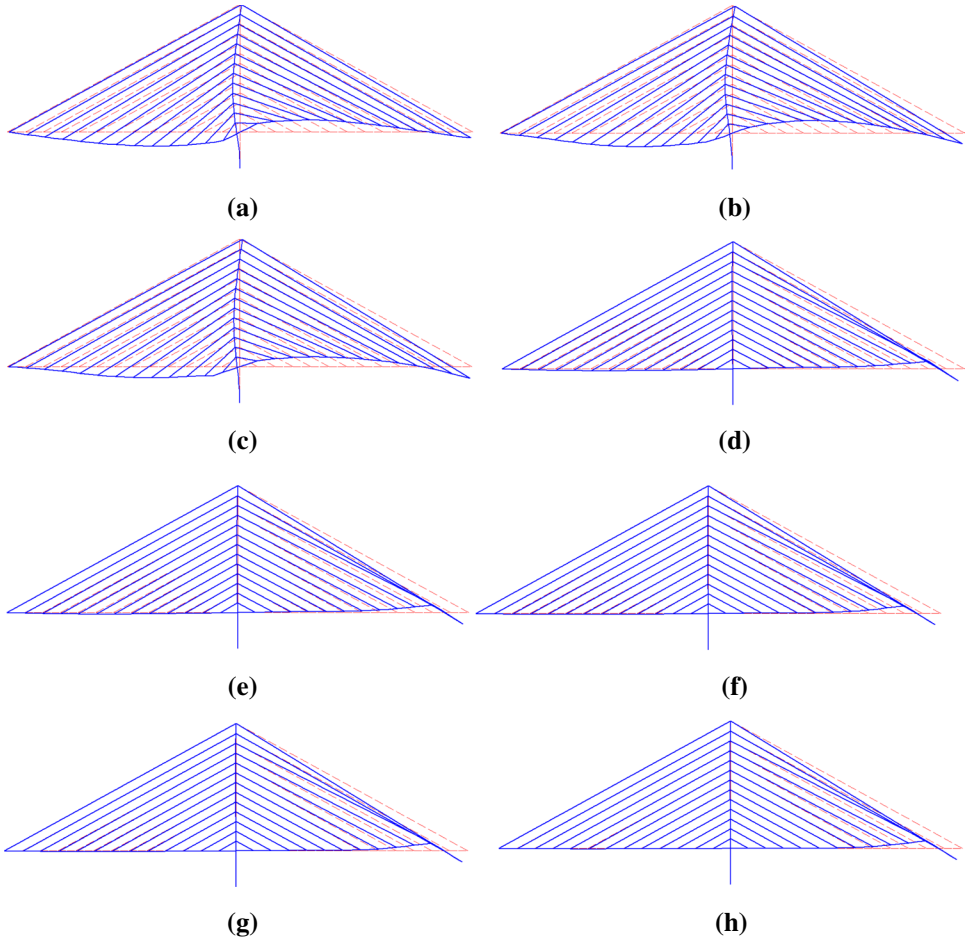

Fig. 21 Ultimate mode shape of harp type models. **a** The stiffness ratio: 2.0. **b** The stiffness ratio: 3.0. **c** The stiffness ratio: 5.0. **d** The stiffness ratio: 7.0. **e** The stiffness ratio: 9.0. **f** The stiffness ratio: 15.0. **g** The stiffness ratio: 20.0. **h** The stiffness ratio: 30.0

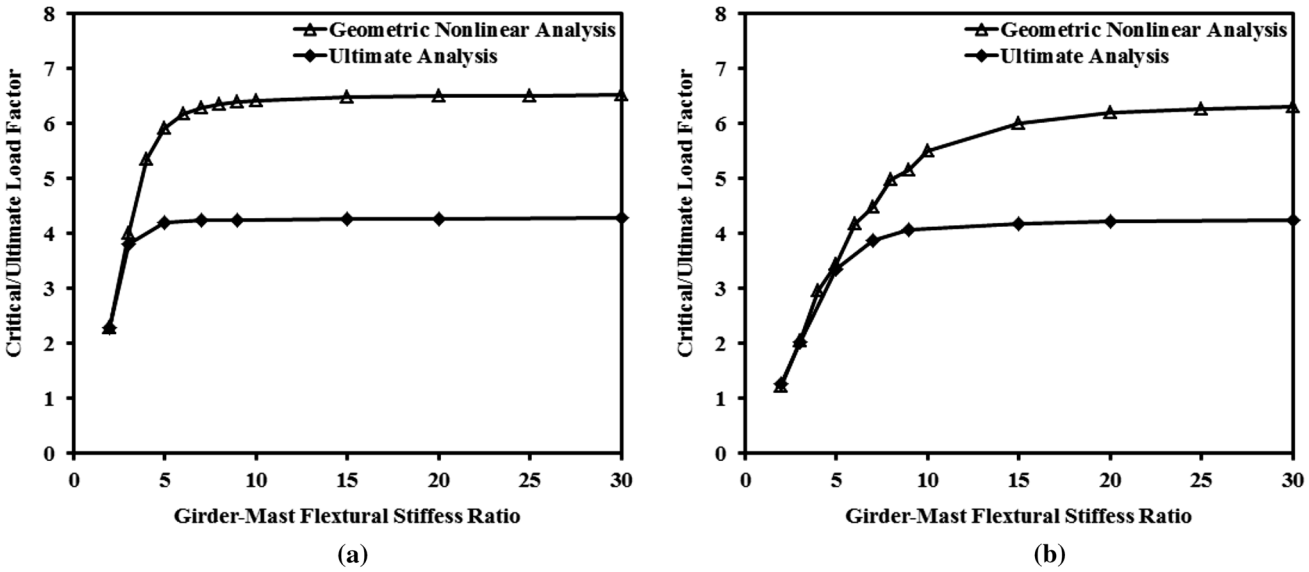

Fig. 22 Critical/ultimate load factor versus girder-mast flexural stiffness ratio. **a** Fan type model. **b** Harp type model

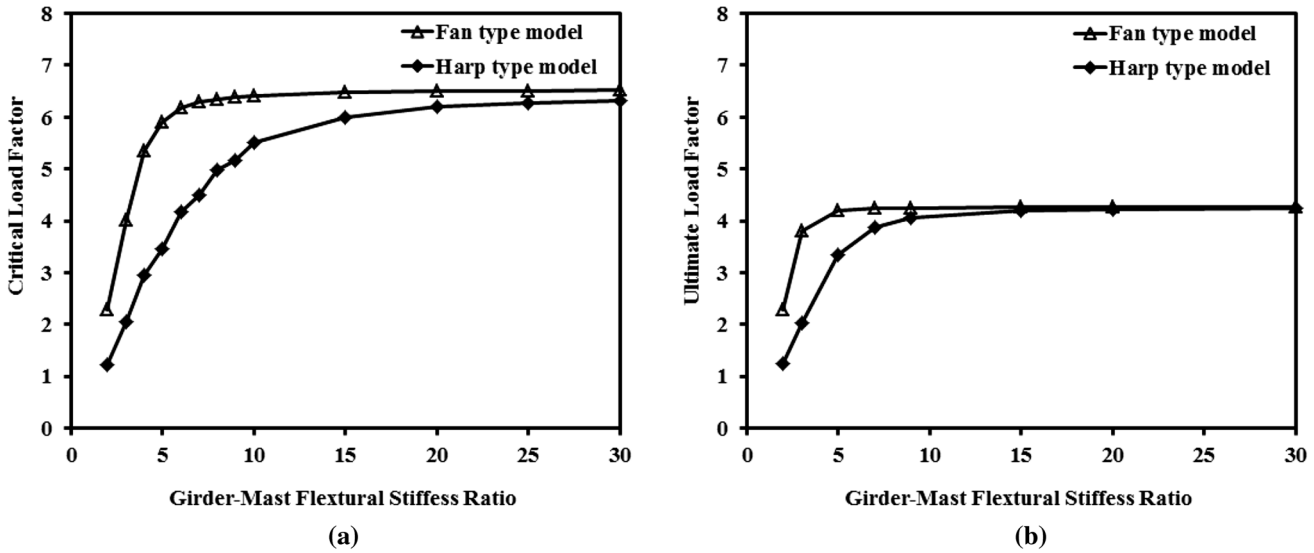

Fig. 23 Fan type versus harp type. **a** Geometric nonlinear analysis. **b** Ultimate analysis

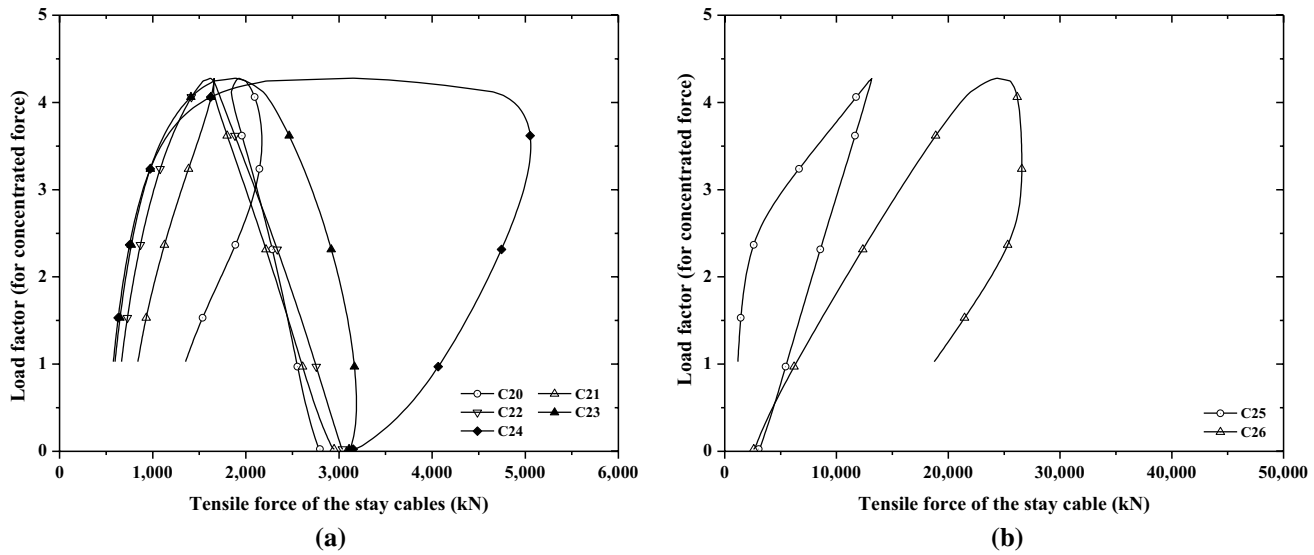

Fig. 24 Load-cable force curve of the fan type model (girder-stiffness ratio: 30.0). **a** C20–C24. **b** C25 and C26

affects the ultimate capacity more than the increase of the weight and sag effect of the cable. The second part shows the decrease of critical load factor as the cable area increases; the contrary can then be said. In this mode, it is concluded that there is optimum cable area that may lead to extreme ultimate capacity under the vertically applied load condition.

In summary, for steel cable-stayed bridges under construction there is a minimum required mast stiffness and optimum cable area that may lead to extreme ultimate load carrying capacity. As mentioned before, when the mast has sufficient flexural stiffness, the girder yield mode becomes the governing buckling mode of steel cable-stayed bridges under construction. In this ultimate mode, the ultimate load factor converges to a specific value, as the flexural stiffness of the mast increases. Moreover, there is an optimum cable area that gives the ultimate load factor a maximum value in this ultimate mode. Therefore, when cable-stayed bridges are designed, their ultimate ability under construction, as well as the completed structure, should be considered and thoroughly studied. This can be achieved by rational stability analysis, like the analysis method proposed in this study.

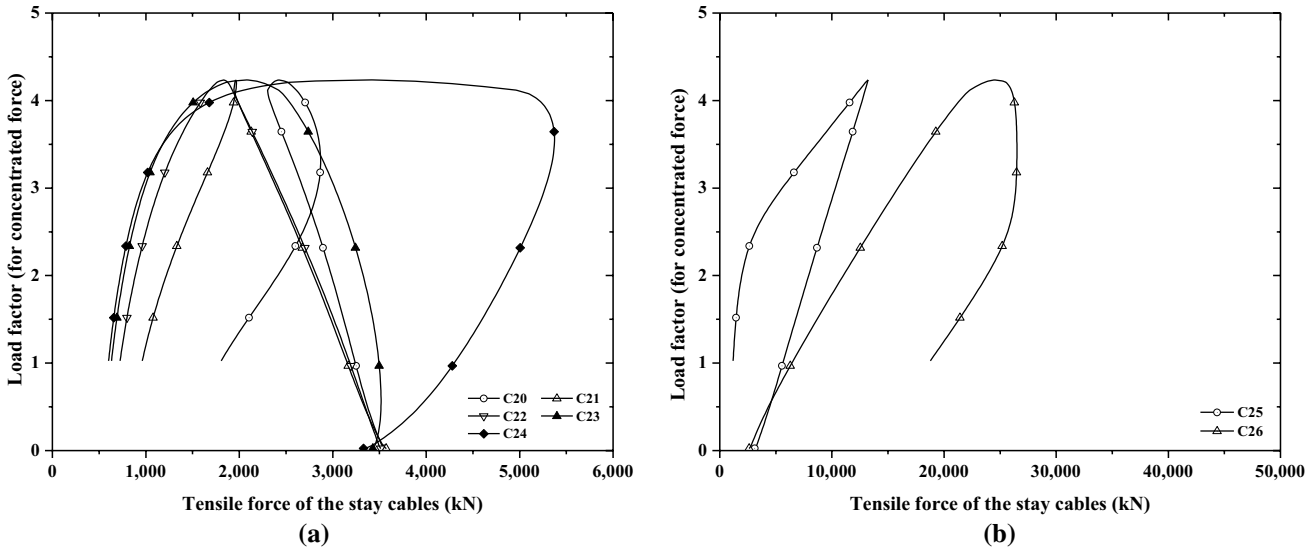

Fig. 25 Load-cable force curve of the harp type model (Girder-stiffness ratio: 30.0). **a** C20–C24. **b** C25 and C26

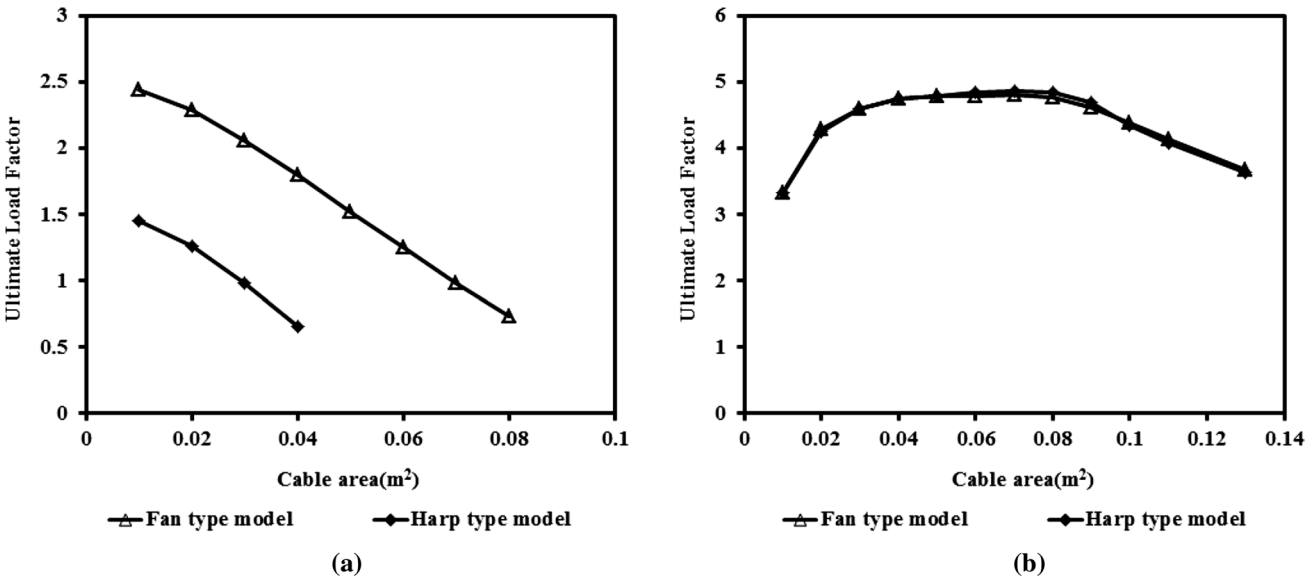

Fig. 26 Sectional area of stay cables versus ultimate load factor. **a** Girder-mast stiffness ratio: 2.0, **b** Girder-mast stiffness ratio: 30.0

4 Conclusion

In this study, the characteristics of the ultimate behavior of steel cable-stayed bridges under construction are investigated, especially for the construction stage before the connection of two individual parts. A rational ultimate analysis method for steel cable-stayed bridges under construction is suggested, based on the theory of nonlinear finite element analysis. Performing the proposed analysis using the program developed in this study, typical buckling modes are classified into two categories, as follows:

1. Girder-mast interactive buckling mode.
2. Girder yield mode.

In fact, the division of inelastic buckling mode wasn't studied in detail. Inelastic buckling might be included in both ultimate modes. The region where both analysis results obtained by geometric nonlinear analysis and ultimate analysis are almost the same can be considered as the elastic buckling region. So, the starting point of the inelastic buckling region can be indicated in the ultimate capacity vs girder-mast stiffness ratio curves. But it is not easy to divide

inelastic buckling from material yield. To determine this, more intensive study is needed.

The effects of girder-mast stiffness ratio, cable arrangement type, and cable area on the ultimate behavior of steel cable-stayed bridges under construction have been investigated by intensive analytical study. Governing ultimate modes are classified for the first time by these analytical studies, and it was found that there are minimum required girder-mast stiffness ratios and optimum cable areas for securing ultimate load carrying capacity under construction.

Acknowledgement This research was supported by a grant (18CTAP-C133500-02) from technology advancement research program funded by Ministry of Land, Infrastructure and Transport of Korean government.

References

Adeli, H., & Zhang, J. (1995). Fully nonlinear analysis of composite girder cable-stayed bridges. *Computers & Structures, 54*(2), 267–277.

Chen, D. W., Au, F. T. K., Tham, L. G., & Lee, P. K. K. (2000). Determination of initial cable forces in prestressed concrete cable-stayed bridges for given design deck profiles using the force equilibrium method. *Computers & Structures, 74,* 1–9.

Cheng, J., & Xiao, R. C. (2004). Probabilistic determination of initial cable forces of cable-stayed bridges under dead loads. *Structural Engineering and Mechanics, 17*(2), 267–279.

Crisfield, M. A. (1983). An arc-length method including line searches and accelerations. *International Journal for Numerical Methods in Engineering, 19,* 1269–1289.

Ernst, H. J. (1965). Der e-modul von seilen unter berucksichtigung des durchanges. *Der Bauingenieur, 40,* 52–55. **(in German)**.

Fleming, J. F. (1979). Nonlinear static analysis of cable-stayed bridges. *Computers & Structures, 10,* 621–635.

Freire, A. M. S., Negrao, J. H. O., & Lopes, A. V. (2006). Geometric nonlinearities on the static analysis of highly flexible steel cable-stayed bridges. *Computers & Structures, 84,* 2128–2140.

Gimsing, N. J. (1983). *Cable supported bridges concept & design* (2nd ed.). New York: Wiley.

Kim, S. (2009). *Ultimate analysis of steel cable-stayed bridges*. Ph.D. dissertation, Korea University, Seoul, Korea.

Kim, S., & Kang, Y. J. (2016). Structural behavior of cable-stayed bridges after cable failure. *Structural Engineering and Mechanics, 59*(6), 1095–1120.

Kim, K. S., & Lee, H. S. (2001). Analysis of target configurations under dead loads for cable-supported bridges. *Computers & Structures, 79,* 2681–2692.

Kim, S., Won, D. H., & Kang, Y. J. (2016a). Ultimate behavior of steel cable-stayed bridges—I. Rational ultimate analysis method. *International Journal of Steel Structures, 16*(2), 601–624.

Kim, S., Won, D. H., & Kang, Y. J. (2016b). Ultimate behavior of steel cable-stayed bridges—II. Parametric study. *International Journal of Steel Structures, 16*(2), 625–636.

Kim, H. J., Won, D. H., Kang, Y. J., & Kim, S. (2017). Structural stability of cable-stayed bridges during construction. *International Journal of Steel Structures, 17*(2), 443–469.

Kim, S., Won, D. H., Lee, K., & Kang, Y. J. (2015). Structural stability of cable-stayed bridges. *International Journal of Steel Structures, 15*(3), 743–760.

Lee, K., Kim, S., Choi, J. H., & Kang, Y. J. (2015). Ultimate behavior of cable stayed bridges under construction: Experimental and analytical study. *International Journal of Steel Structures, 15*(2), 311–318.

Liew, J. Y. R., White, D. W., & Chen, W. F. (1993). Second order refined plastic-hinge analysis for frame design. Part I. *Journal of Structural Engineering, 119*(11), 3196–3216.

Lim, N. H., Han, S. Y., Han, T. H., & Kang, Y. J. (2008). Parametric study on stability of continuous welded rail track—ballast resistance and track irregularity. *International Journal of Steel Structures, 8*(3), 171–181.

Reddy, P., Ghaboussi, J., & Hawkins, N. M. (1999). Simulation of construction of cable-stayed bridges. *Journal of Bridge Engineering, ASCE, 4*(4), 249–257.

Ren, W. X. (1999). Ultimate behavior of long-span cable stayed bridges. *Journal of Bridge Engineering, ASCE, 4*(1), 30–36.

Shu, H. S., & Wang, Y. C. (2001). Stability analysis of box-girder cable-stayed bridges. *Journal of Bridge Engineering, ASCE, 6*(1), 63–68.

Song, W. K., & Kim, S. E. (2007). Analysis of the overall collapse mechanism of cable-stayed bridges with different cable layouts. *Engineering Structures, 29,* 2133–2142.

Song, M. K., Kim, S. H., & Choi, C. K. (2006). Enhanced finite element modeling for geometric non-linear analysis of cable-supported structures. *Structural Engineering and Mechanics, 22*(5), 575–597.

Tang, C. C., Shu, H. S., & Wang, Y. C. (2001). Stability analysis of steel cable-stayed bridge. *Structural Engineering and Mechanics, 11*(1), 35–48.

Wang, P. H., Tang, T. Y., & Zheng, H. N. (2004). Analysis of cable-stayed bridges during construction by cantilever methods. *Computers & Structures, 82,* 329–346.

Wang, P. H., Tseng, T. C., & Yang, C. G. (1993). Initial shape of cable stayed bridge. *Computers & Structures, 47*(1), 111–123.

Wang, P. H., & Yang, C. G. (1996). Parametric studies on cable stayed bridges. *Computers & Structures, 60*(2), 243–260.

Xi, Y., & Kuang, J. S. (1999). Ultimate load capacity of cable-stayed bridges. *Journal of Bridge Engineering, ASCE, 4*(10), 14–22.

Yang, Y. B., & Kuo, S. R. (1994). *Theory and analysis of nonlinear framed structures*. Singapore: Prentice-Hall Inc.